Article

Cell Reports

Genomic *DISC1* Disruption in hiPSCs Alters Wnt Signaling and Neural Cell Fate

Graphical Abstract

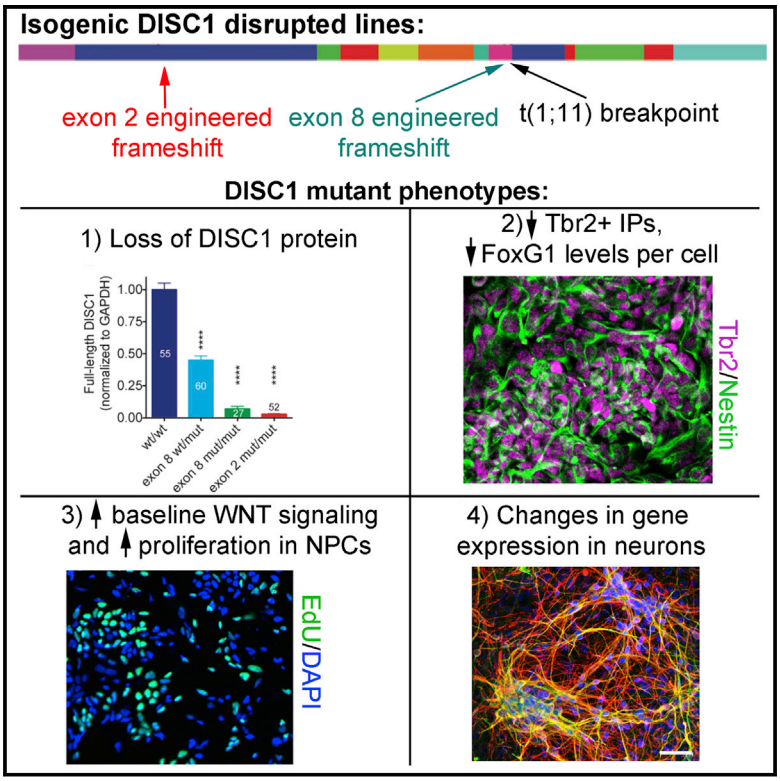

Highlights

- We generate isogenic human iPSCs with an engineered disruption of the *DISC1* gene
- *DISC1* disruption results in decreased expression of long DISC1 isoforms
- *DISC1* disruption affects the expression of NPC fate markers, including FoxG1 and Tbr2
- *DISC1* mutant NPCs show elevated baseline Wnt signaling and proliferation

Authors

Priya Srikanth, Karam Han, Dana G. Callahan, ..., Kenneth S. Kosik, Dennis J. Selkoe, Tracy L. Young-Pearse

Correspondence

tyoung@rics.bwh.harvard.edu

In Brief

Srikanth et al. report the generation of isogenic hiPSC lines with engineered mutations in two locations within the *DISC1* gene. This disease-relevant disruption shows a loss of long isoforms, which, in turn, affects neural progenitor cell proliferation, baseline WNT signaling, and the expression of NPC fate markers such as FoxG1 and Tbr2.

Accession Numbers

GSE71289

Srikanth et al., 2015, Cell Reports *12*, 1414–1429
September 1, 2015
http://dx.doi.org/10.1016/j.celrep.2015.07.061

OPEN ACCESS
CellPress

Cell Reports
Article

Genomic *DISC1* Disruption in hiPSCs Alters Wnt Signaling and Neural Cell Fate

Priya Srikanth,[1,2,3] Karam Han,[1] Dana G. Callahan,[1] Eugenia Makovkina,[1] Christina R. Muratore,[1] Matthew A. Lalli,[4] Honglin Zhou,[4] Justin D. Boyd,[1] Kenneth S. Kosik,[4] Dennis J. Selkoe,[1] and Tracy L. Young-Pearse[1,*]
[1]Ann Romney Center for Neurologic Diseases, Brigham and Women's Hospital and Harvard Medical School, Boston, MA 02115, USA
[2]Program in Neuroscience, Harvard Medical School, Boston, MA 02115, USA
[3]Harvard MD-PhD Program, Harvard Medical School, Boston, MA 02115, USA
[4]Neuroscience Research Institute, Department of Molecular Cellular and Developmental Biology, Biomolecular Science and Engineering Program, University of California, Santa Barbara, Santa Barbara, CA 93106, USA
*Correspondence: tyoung@rics.bwh.harvard.edu
http://dx.doi.org/10.1016/j.celrep.2015.07.061

SUMMARY

Genetic and clinical association studies have identified disrupted in schizophrenia 1 (*DISC1*) as a candidate risk gene for major mental illness. *DISC1* is interrupted by a balanced chr(1;11) translocation in a Scottish family in which the translocation predisposes to psychiatric disorders. We investigate the consequences of *DISC1* interruption in human neural cells using TALENs or CRISPR-Cas9 to target the *DISC1* locus. We show that disruption of *DISC1* near the site of the translocation results in decreased DISC1 protein levels because of nonsense-mediated decay of long splice variants. This results in an increased level of canonical Wnt signaling in neural progenitor cells and altered expression of fate markers such as Foxg1 and Tbr2. These gene expression changes are rescued by antagonizing Wnt signaling in a critical developmental window, supporting the hypothesis that DISC1-dependent suppression of basal Wnt signaling influences the distribution of cell types generated during cortical development.

INTRODUCTION

Schizophrenia and other major mental illnesses (MMIs) are widely regarded to result from a combination of genetic susceptibility and environmental insults. Clinical and genetic studies indicate that schizophrenia and other MMIs are likely diseases of altered circuitry resulting from disruptions in neurodevelopment (Harrison, 1999; Weinberger, 1995; Williams et al., 2009). The recent expansion of genome-wide association studies (GWASs) has identified many interesting but generally weak genetic linkages to MMI (Cross-Disorder Group of the Psychiatric Genomics Consortium, 2013; Ripke et al., 2013; Schizophrenia Working Group of the Psychiatric Genomics Consortium, 2014). There are also rare strong genetic variants that have been associated with mental illness, including various copy number variants (CNVs) and mutation of the gene disrupted in schizophrenia 1 (*DISC1*) (Millar et al., 2000; Mitchell, 2011; Sullivan et al., 2012). *DISC1* was initially associated with mental illness upon the discovery that its coding sequence is interrupted by a balanced chr(1;11) translocation in a Scottish family in which the translocation cosegregates with schizophrenia, bipolar disorder, and major depression (Blackwood et al., 2001; Millar et al., 2000; St Clair et al., 1990). The diversity of phenotypes in subjects harboring the translocation supports the hypothesis that the translocation leads to a subtle underlying disruption in neural development that predisposes to MMI by increasing vulnerability to other environmental and genetic risk factors. Although such rare variants are not likely to contribute significantly to the incidence of sporadic disease, they offer valuable opportunities for investigation. Here we engineered a disease-relevant disruption of the *DISC1* locus in an isogenic background to investigate whether and how *DISC1* mutation might lead to a subtle underlying disruption in development that predisposes to MMI.

DISC1 has been implicated in several neurodevelopmental processes, including proliferation, synaptic maturation, neurite outgrowth, and neuronal migration. In addition, many known DISC1-interacting proteins have been associated independently with neuropsychiatric diseases, further implicating this network of proteins in the pathophysiology of mental illness (reviewed in Brandon and Sawa, 2011). The vast majority of studies showing functions of DISC1 in neural development were performed in rodents. Dozens of splice variants of *DISC1* have been identified in the developing human brain (Nakata et al., 2009), and the architecture of splice variant expression is not identical in humans and rodents (Ma et al., 2002; Taylor et al., 2003). The evolutionary divergence of cerebral cortex development in humans and rodents, coupled to differences at the *DISC1* locus between species, highlights the importance of interrogating the effects of disease-relevant disruption of *DISC1* isoforms in a model of human neurodevelopment.

Here we study the consequences of *DISC1* disruption in isogenic stem cell lines generated using transcription activator-like effector nucleases (TALENs) or clustered regularly interspaced short palindromic repeats (CRISPR)-Cas9 to interrupt *DISC1* near the site of the balanced translocation or in an exon common to all isoforms. Multiple isogenic clonal lines are compared for each genotype, allowing careful study of the effects of genomic *DISC1* interruption on gene expression and neuronal development. We show that disease-relevant *DISC1* targeting decreases DISC1 protein expression, which, in turn, results in increased Wnt signaling in neural progenitor cells and changes in expression of markers of cell fate. DISC1-dependent Wnt signaling and changes in expression of cell fate markers can be reversed by antagonizing the Wnt pathway during a critical window in neural progenitor development. These experiments suggest that disruption of long *DISC1* isoforms results in elevated basal Wnt signaling, which alters the identity of neural progenitors, thereby modifying Wnt responsiveness and neuronal identity. The data in this study identify the effects of *DISC1* disruption on human cerebral cortical development, shedding light on the functions of DISC1 relevant to the pathogenesis of major mental illness.

RESULTS

Genomic *DISC1* Exon 8 Interruption Results in Loss of DISC1 Expression because of Nonsense-Mediated Decay

To investigate the effects of *DISC1* interruption at the site of the Scottish translocation, we introduced *DISC1* frameshift mutations into control induced pluripotent stem cells (iPSCs). Mutations were introduced into exon 8 (within ten codons of the site of the translocation) or exon 2 (intended to disrupt all known coding isoforms) (Figure 1). Using TALENs or CRISPR-Cas9, we generated isogenic human iPSC lines that are wild-type (WT) or have frameshift mutations in exon 8 (monoallelic, exon 8 WT/mut or ex8wm; biallelic, exon 8 mut/mut or ex8mm) or exon 2 (biallelic, exon 2 mut/mut or ex2mm). In the chr(1;11) balanced translocation, splicing of DISC1 exon 8 to the next two available exons on chr11 results in the introduction of a premature stop codon (PTC) within two or 61 codons. Exon 8 targeting generated indels that result in a PTC within three codons (exon 8 ins 1 bp) or 27 codons (exon 8 del 1 bp). Similarly, exon 2 targeting yielded biallelic indels, resulting in a PTC within 12 codons (exon 2 ins 1 bp) or 65 codons (exon 2 ins 2 bp). Targeted cells maintained iPSC colony morphology, expressed iPSC markers (Figure 1E; Figure S1), and maintained a euploid karyotype (Figure S2). No predicted off-target cleavage events were detected using RNA sequencing (Supplemental Experimental Procedures). Multiple iPSC clones of each genotype were used for the studies described here to minimize the potential effects of clonal variability (Table S1).

Genomic *DISC1* interruption has been hypothesized to cause expression of a truncated or mutant DISC1 or to decrease DISC1 expression from the mutated allele (Brandon and Sawa, 2011). The introduction of a PTC into a coding RNA often results in nonsense-mediated decay (NMD) if the PTC occurs prior to the last exon-exon junction of the transcript (Silva and Romão, 2009). Therefore, we hypothesized that genomic *DISC1* interruption would cause the decay of PTC-containing mRNAs that extended at least one exon past the interruption. Given the complexity of human *DISC1* splicing (Nakata et al., 2009), we chose to analyze transcription at multiple *DISC1* coding regions.

To examine the effects of genomic *DISC1* interruption on *DISC1* expression, RNA was harvested from neural precursor cells (NPCs) and differentiated neurons. Wild-type and *DISC1*-targeted iPSCs were differentiated to neural fates using an embryoid aggregate-based protocol (Muratore et al., 2014a, 2014b), which results in definitive neuroepithelium by day 17 and expression of neuronal makers after day 25. We characterized the expression of multiple isoforms of *DISC1* by examining the RNA expression of distinct exons. Day 40 neuronal qPCR analyses revealed that the presence of a single exon 8 mutant allele did not significantly decrease *DISC1* exon 2 expression but did decrease expression of the longest *DISC1* isoforms (Figures 2A and 2B). Biallelic exon 8 interruption significantly decreased *DISC1* exon 2 and long *DISC1* transcripts (Figures 2A and 2B). Surprisingly, biallelic exon 2 mutation did not reduce *DISC1* expression (Figure 2A). We further investigated the levels of various *DISC1* isoforms in NPCs (day 17) and neurons (day 50) using a custom NanoString probeset that included probes targeting multiple *DISC1* exons. The NanoString analyses confirmed the qPCR data, where introduction of a PTC into exon 8 decreased the expression of longer but not shorter *DISC1* transcripts on days 17 and 50 (Figure 2C). Unexpectedly, exon 2 targeting appeared to decrease *DISC1* expression on day 17 (Figure 2C) but either did not change or increased the expression of various *DISC1* isoforms on days 40–50 (Figures 2A–2C).

To investigate the effects of *DISC1* interruption at the protein level, we performed western blots of day 40 neuronal lysates and analyzed DISC1 expression using a monoclonal antibody generated against the C terminus of DISC1. This antibody detected a single band of approximately 85 kDa, roughly corresponding to the predicted molecular weight of translated long (or "full-length") *DISC1* isoforms (L, 854 amino acids [aa]; Lv, 832 aa). Single allelic DISC1 exon 8 mutation resulted in an ~55% decrease in DISC1 protein expression, whereas biallelic exon 8 mutation led to total loss of detectable DISC1 protein (Figures 2D–2F). Biallelic exon 2 targeting showed a total loss of full-length protein but, unexpectedly, led to the expression of a shorter, novel DISC1 protein product in day 40 neural cells (Figure 2D, red arrows). This truncated protein was expressed at levels nearly identical to that of wild-type, long-isoform DISC1 (Figure 2F). Although unexpected, the truncated DISC1 protein resulting from exon 2 mutation provided an opportunity to analyze the effects of an independent *DISC1* mutation in a system that was isogenic to our disease-relevant (exon 8 disruption) model. Because several prior studies have demonstrated that misexpression of a mutant-truncated DISC1 can phenocopy *DISC1* knockdown (reviewed in Brandon and Sawa, 2011), we used our exon 2- and exon 8-targeted cells to explore whether these observations would hold true in a human neuronal context.

To determine whether the observed changes in *DISC1* expression in the disease-relevant exon 8-targeted cells were due to NMD of PTC-containing mRNAs, we treated day 40 neurons with cycloheximide (CHX), which inhibits NMD by interfering

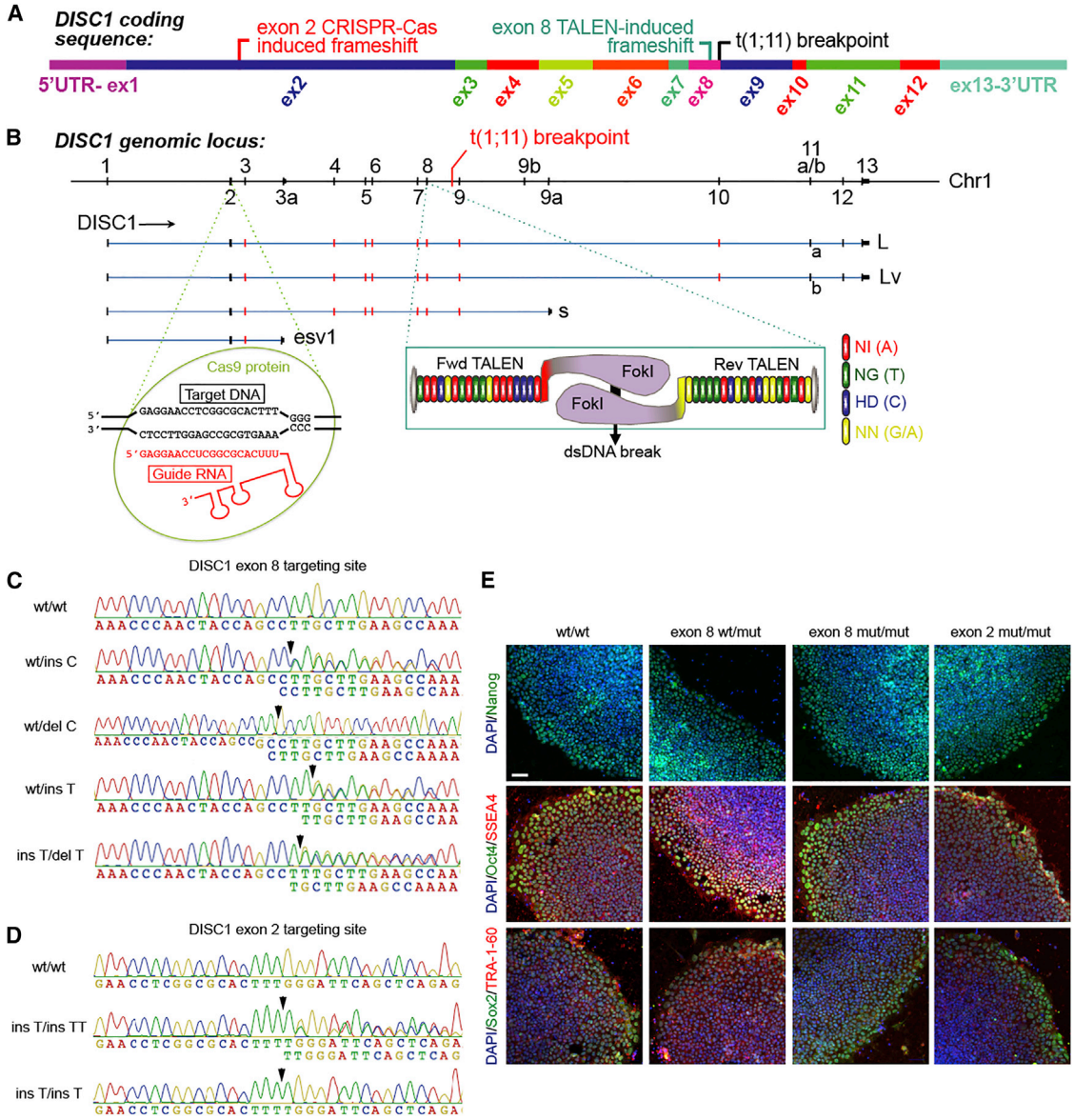

Figure 1. Genome Editing of the Human *DISC1* Locus

(A) Diagram of the coding sequence of *DISC1*, with the sites of induced frameshifts and the Scottish chr(1;11) translocation indicated.

(B) Diagram of the *DISC1* genomic locus, with exons shown on the top line and sample transcripts shown below. A selection of alternatively spliced isoforms is shown in red.

(C and D) Wild-type and mutant sequences around the exon 8 (C) or exon 2 (D) targeting sites, obtained by Sanger sequencing of targeted iPS colonies. Mutation sites are indicated with black arrowheads.

(E) Immunostaining for the pluripotent cell markers Nanog, Oct4, SSEA4, Sox2, and TRA-1-60 following genome editing. Scale bar, 50 μm.

See also Figure S1.

with the "pioneer" round of translation required to detect the PTC (Ishigaki et al., 2001). Analysis of *DISC1* expression after CHX treatment revealed significantly increased NMD in exon 8- but not exon 2-targeted cells (Figures 2G and 2H). These data suggest that introduction of a PTC into *DISC1* exon 8, but not exon 2, results in NMD of PTC-containing transcripts.

We further explored the effects of *DISC1* genomic disruption on DISC1 protein stability using CHX to prevent translation in day 40 neurons. DISC1 protein was remarkably refractory to turnover under these conditions, showing very little or no degradation over 24 hr and no significant alteration in protein stability with exon 8 or exon 2 mutations (Figure S3). The efficacy of the CHX treatment was confirmed by detecting APP levels, which showed a half-life of ~4 hr for this protein, in agreement with previous reports (Lefort et al., 2012; Vieira et al., 2010). These results suggest that DISC1 exon 8 mutation results in NMD of longer

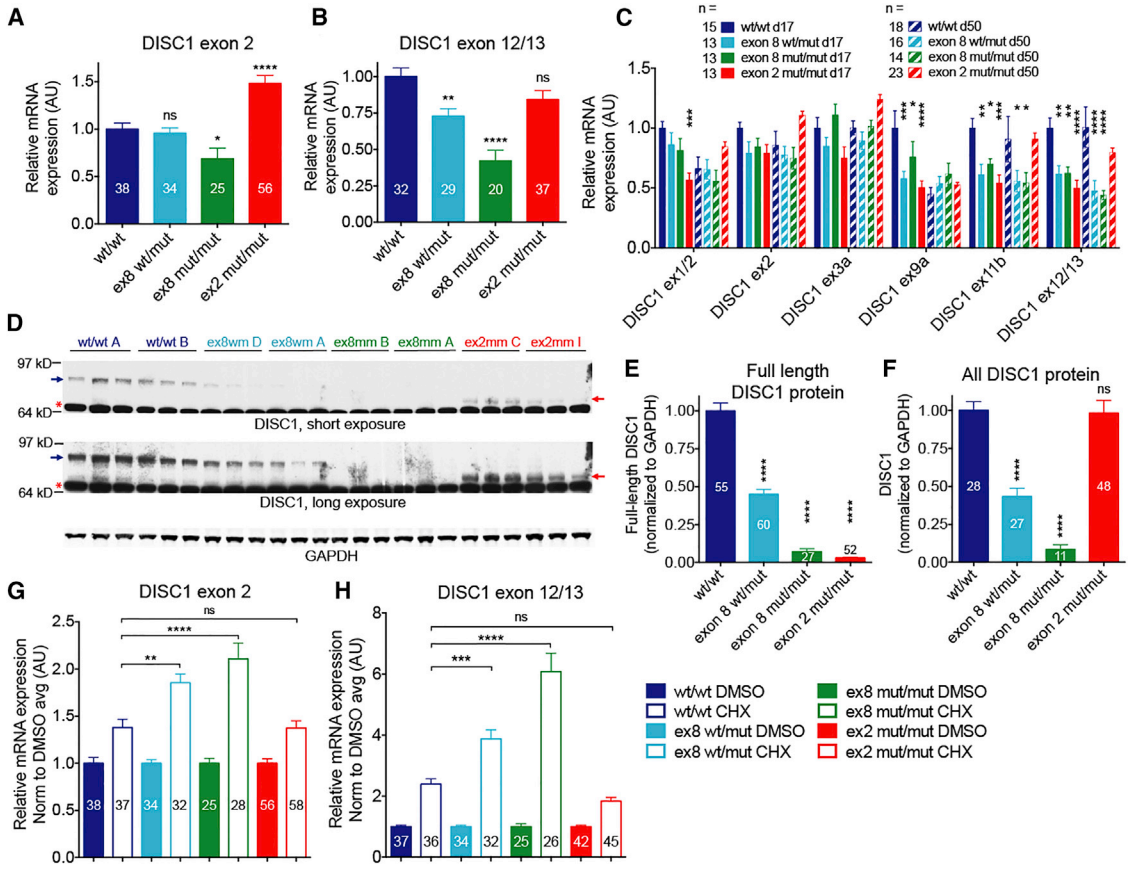

Figure 2. *DISC1* Exon 8 Disruption Causes Loss of Full-Length *DISC1* Expression via NMD

(A and B) Wild-type and DISC1-disrupted iPSCs were differentiated to day 40 neural fates, and RNA was harvested for qRT-PCR of *DISC1* exon 2 (*A*) or exons 12/13 (*B*). Expression is normalized to *GAPDH* and WT/WT levels. AU, arbitrary unit.

(C) iPSCs were differentiated to NPCs (day 17) and neurons (day 50), and RNA was harvested for NanoString. *DISC1* probe expression was normalized to expression of eight housekeeping genes and average WT/WT day 17 levels. Statistics are shown versus the WT of the corresponding differentiation day.

(D) Representative western blot of DISC1 in day 40 neuronal lysates. Full-length DISC1 is indicated with blue arrows. Novel truncated DISC1 is indicated by red arrows. The red asterisks denote a nonspecific band.

(E and F) Quantification of full-length (E) or all (F) DISC1 from western blots of day 40 neuronal lysates, normalized to GAPDH and WT/WT levels.

(G and H) Day 40 neurons were treated with 100 μg/ml CHX or vehicle (DMSO) for 3 hr, followed by RNA harvest and qRT-PCR for exon 2 (G) or the exon 12/13 junction (H) of *DISC1*. Expression was normalized to *GAPDH* and average DMSO expression within the genotype.

All data were derived from at least five independent differentiations, and n is shown for each panel within bars or in the legend. Statistics: two-way ANOVA (C) and one-way ANOVA (A, B, and E–H); mean ± SEM is shown; ns, not significant; *p < 0.05 **p < 0.01, ***p < 0.001, ****p < 0.0001. See also Figure S3.

DISC1 transcripts and that exon 2 mutation causes expression of an N-terminally truncated DISC1 but that neither mutation destabilizes DISC1 protein.

Genomic *DISC1* Interruption Alters the Expression of NPC Fate Markers

To examine the broader effects of *DISC1* disruption, we characterized gene expression profiles and cell fate in wild-type and *DISC1*-targeted NPCs. Neural differentiation resulted in the expression of transcription factors consistent with dorsal forebrain NPC fates across all genotypes on day 17 (Figure 3A). To quantitatively measure the expression of a broad selection of neural markers, we used a custom NanoString codeset to assay RNA expression in rosette-selected day 17 NPCs. NanoString analyses showed that *DISC1* exon 8 and exon 2 interruption significantly decreased *FoxG1* and *Tbr2* (*EOMES*) expression (Figure 3B). There was also decreased Sox1 and increased Pax6 expression in exon 2-targeted NPCs, suggesting that exon 2 mutation causes more dramatic changes than exon 8 interruption (Figures 3B and 3C). *DISC1* interruption did not alter the expression of other broad progenitor markers, such as *Sox2*, *HES1*, *Nestin* (*NES*), or *Vimentin* (*VIM*) (Figures 3B and 3C). The decrease in *FoxG1* and *Tbr2* RNA in the absence of decreased expression of other cortical progenitor markers argued against a deficit in telencephalic differentiation.

To explore putative changes in the percentage of cells expressing FoxG1 and Tbr2, we quantified immunostaining in wild-type NPCs and NPCs with our disease model mutation, DISC1 exon 8 WT/mut. Tbr2 quantification revealed a significant decrease in the percentage of Tbr2-expressing cells (Figure 3D),

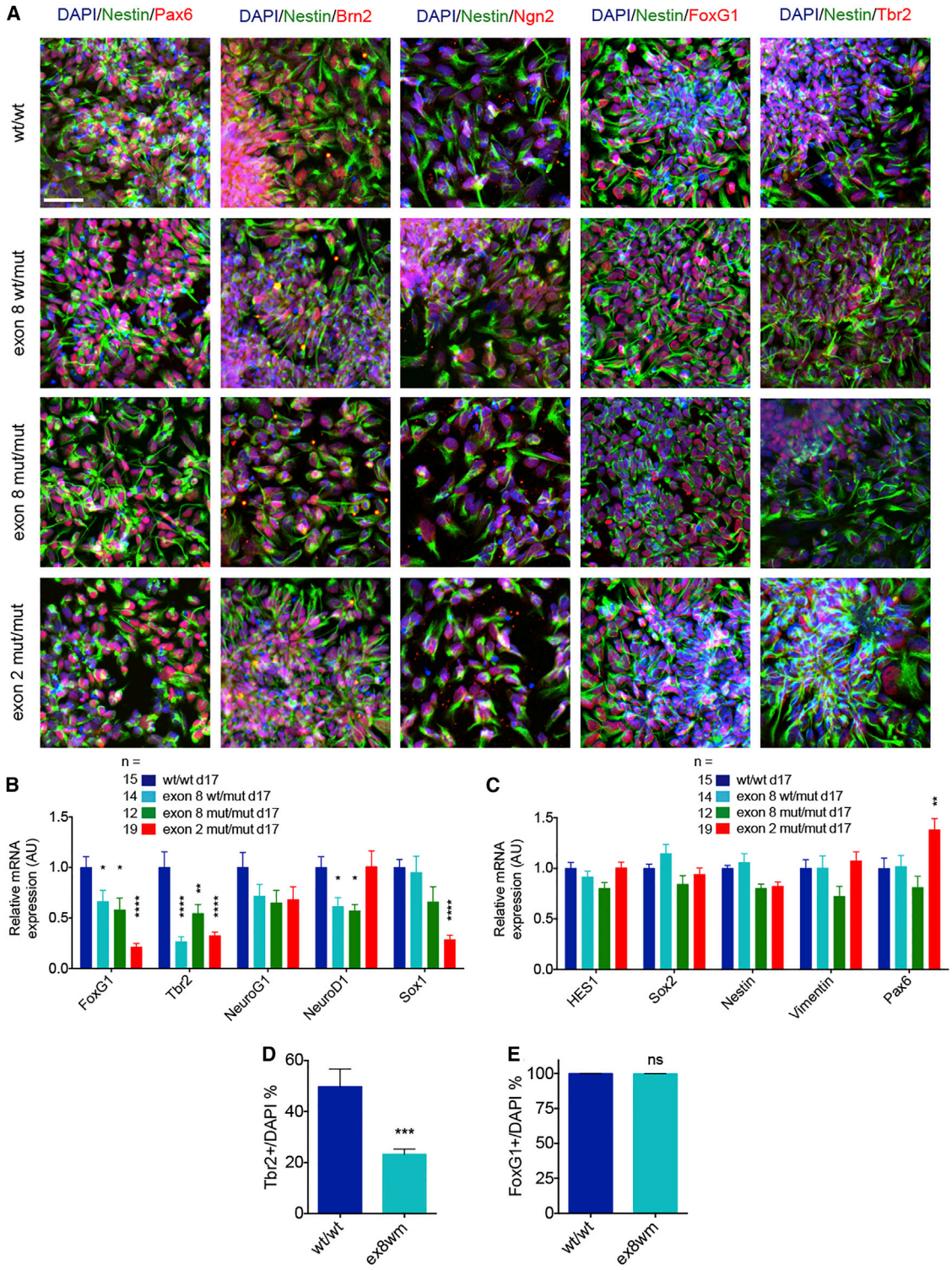

Figure 3. *DISC1* Disruption Causes Subtle Alterations in NPC Fate

(A) iPSCs were differentiated to day 17 NPCs, rosette-selected, plated for 48 hr, and immunostained for the NPC markers as shown. Scale bar, 50 μm. DAPI, 4′,6-diamidino-2-phenylindole.

(B and C) iPSCs were differentiated to day 17 NPCs and rosette-selected, and RNA was harvested for NanoString. Gene expression was normalized to expression of eight housekeeping genes and WT/WT levels.

(legend continued on next page)

demonstrating that the decreased *Tbr2* RNA expression reflects fewer Tbr2+ cells. In contrast, although *FoxG1* RNA expression was also decreased by *DISC1* disruption, immunostaining quantification revealed that nearly 100% of NPCs expressed FoxG1 regardless of *DISC1* mutation status (Figure 3E). This indicates that the *FoxG1* gene expression data reflect a per-cell decrease in expression' rather than a decrease in the number of FoxG1+ cells.

DISC1 Interruption Subtly Alters Neuronal Fate but Not Neuronal Maturity

We further investigated effects of *DISC1* disruption on the expression of cell fate markers in iPSC-derived neurons. Differentiation for 40 days resulted in marker expression characteristic of lower- and upper-layer neurons (CTIP2, Tbr1, Cux1, Brn2, and Satb2) as well as general neuronal markers (Tau and MAP2; Figure 4A). A population of NPCs persisted in these cultures (Nestin and Tbr2; Figure 4A). Neural cultures of all genotypes demonstrated spontaneous action potentials by day 42 when co-cultured with astrocytes (Figures 4B and 4C). Gene expression was assayed in day 50 neurons by NanoString, revealing a persistent decrease in *Tbr2* and *FoxG1* in DISC1-disrupted neurons (Figure 4D). There were no significant expression changes of general neuronal markers (Figure 4E). Exon 2 mut/mut neurons expressed lower levels of the select mature neuronal genes *VGLUT1* (*SLC17A7*), *GRIN1*, and *MAP2* (Figure 4F). Exon 8 interruption did not significantly alter neuronal layer marker expression, whereas exon 2 interruption significantly decreased expression of the cortical neuronal markers *CTIP2* (*BCL11B*), *FezF2*, and *Tbr1*, with a trend for decreased expression of other cortical markers (*Satb1* and *Cux1*) (Figure 4F). These gene expression changes support the day 17 NPC data, where exon 8 interruption subtly affects the expression of cell fate markers without impairing neuronal differentiation and exon 2 interruption causes a broader dysregulation of neurogenesis.

We further investigated neuronal maturity by assessing the expression of presynaptic proteins. Western blot analyses revealed no significant alterations in SYP or Syn I expression with *DISC1* disruption (Figures 4G–4I), in contrast to a different clinical *DISC1* mutation (exon 12 Δ4bp; Sachs et al., 2005), which has been found to result in a dramatic increase in both (Wen et al., 2014).

RNA Sequencing Supports a Shift in Gene Expression Profiles toward Dorsal Identities in *DISC1*-Interrupted NPCs and Neurons

To obtain a genome-wide view of gene expression changes, we performed RNA sequencing (RNA-seq) on day 17 NPC samples and day 50 neuronal samples of wild-type and *DISC1*-disrupted cells. These data show that interruption at exon 8 did not alter global gene expression as dramatically as at exon 2 (Figure 5; Figure S4; Table S2). Examination of cell fate markers largely confirmed and extended the NanoString findings, suggesting a subtle shift in the expression of cell fate markers with *DISC1* interruption (Figure 5), including decreased *FoxG1* expression in *DISC1*-disrupted NPCs (Figure 5D). To investigate potential dorsal-ventral fate shifts, we evaluated the expression of a subset of dorsal and ventral markers. Because the "default" neuronal differentiation pathway of human stem cells generates dorsal excitatory cortical neurons (Espuny-Camacho et al., 2013; Kim et al., 2011; Li et al., 2009), many markers characteristic of ventral or interneuron progenitors were not expressed in these cells (less than ten reads in ten samples, including *NKX2-1*, *NKX2-2*, *NKX6-2*, and *FOXA2*). Among telencephalic progenitor markers, expression of a selection of roof plate and dorsal progenitor markers was increased (*Pax3*, *Pax7*, *Msx2*, *NeuroG2*, *Dbx2*, and *Wnt8B*), and expression of ventral progenitor markers was decreased (*ASCL1*, *DLX1*, *DLX2*, and *Gsx2*), by *DISC1* interruption (Figures 5A and 5B). Notably, *Pax3*, *Pax7*, *NeuroG2*, *Msx2*, *Dbx2*, *Wnt8B*, *ASCL1*, *DLX1*/2, *GSX2*, *FoxG1*, and *Tbr2* were identified in transcriptome-wide comparisons (Table S2). Although this RNA-seq analysis was limited by low sample numbers, it supports a subtle dorsal shift in cell fate with *DISC1* interruption.

Gene ontology analysis identified genes involved in neural development, mental disorders, schizophrenia, Wnt signaling, cell adhesion, and other pathways as being altered significantly in our exon 8 WT/mut disease model on days 17 or 50 (Figures 5G–5J). Comparison of differentially expressed genes across genotypes and with other existing datasets also highlights priority genes for future study based on their involvement in another model of DISC1-related mental illness (Wen et al., 2014) or in human neural progenitor development (Johnson et al., 2015; Figures S4E–S4G).

The observed changes in gene expression suggested that disease-relevant *DISC1* exon 8 interruption did not drastically alter neuronal differentiation capacity or neuronal maturation but did result in significant changes in gene expression, including decreased *FoxG1* and *Tbr2* expression. FoxG1 is a marker of telencephalic progenitors (Molyneaux et al., 2007; Shimamura et al., 1995; Tao and Lai, 1992; Xuan et al., 1995), whereas Tbr2 is expressed in intermediate progenitor (IP) cells of the cortex (Englund et al., 2005; Hevner et al., 2006; Sessa et al., 2008). Although FoxG1 is expressed broadly in progenitor cells of the developing neocortex, it is particularly critical for the differentiation of ventral forebrain neurons (Manuel et al., 2010; Martynoga et al., 2005; Xuan et al., 1995) and is expressed in a high-ventral to low-dorsal gradient in the developing forebrain (Danesin et al., 2009).

We hypothesized that *DISC1* disruption might subtly alter neural cell fate via an established patterning pathway. The Wnt proteins are a major family of patterning molecules that are present in a dorsal-to-ventral gradient and act on neural progenitors to create a dorsal neuronal population (Ulloa and Martí, 2010).

(D and E) NPCs were immunostained for Tbr2 (D) or FoxG1 (E) and co-stained with DAPI. The percentage of Tbr2- or FoxG1-expressing cells was calculated using the Cell Counter plugin in FIJI. Only Nestin-positive cells were counted. The cells were counted as follows: Tbr2, 3,916 (WT/WT) and 5,873 (ex8wm); FoxG1, 5,921 (WT/WT) and 5,424 (ex8wm).

Data were derived from at least five independent differentiations. Statistics: two-way ANOVA (B and C) and two-tailed Student's t test (D and E). Mean ± SEM is shown. *$p < 0.05$, **$p < 0.01$, ****$p < 0.0001$.

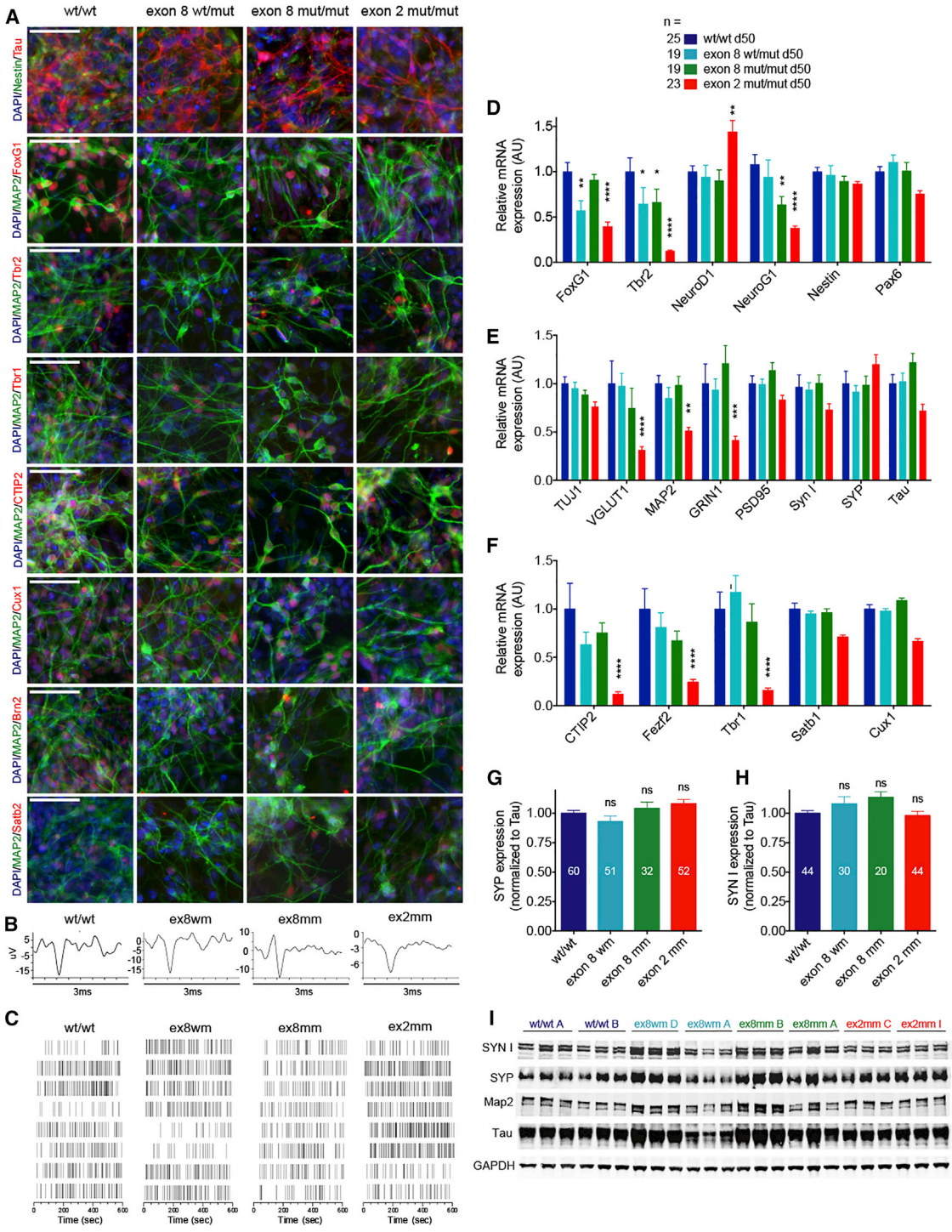

Figure 4. *DISC1* Disruption Does Not Alter Neuronal Differentiation Capacity or Maturity but Causes Subtle Alterations in Cell Fate

(A) iPSCs were differentiated to day 40 neuronal fates and immunostained for the markers labeled. Scale bars, 50 μm.

(B and C) Day 24 cells were dissociated and plated with human astrocytes on microelectrode arrays.

(B) Examples of day 42 single unit waveforms.

(C) Example raster plots from day 47 neurons. Each row represents one electrode. Eight representative electrodes were selected from one recording of each of the genotypes as shown.

(D–F) iPSCs were differentiated to day 50 neuronal fates, and RNA was harvested for NanoString. Gene expression was normalized to expression of eight housekeeping genes and WT/WT levels.

(legend continued on next page)

Artificially elevating Wnt signaling in the developing rodent cortex has been shown to decrease FoxG1 expression and cause a dorsal shift in neural identity (Backman et al., 2005). Wnts have also been shown to trigger IP differentiation and premature neuronal differentiation, therefore reducing the abundance of Tbr2-positive cells in the cortex (Hirabayashi et al., 2004; Munji et al., 2011). Finally, DISC1 has been shown to participate in the Wnt signaling pathway via interactions with GSK3β (Mao et al., 2009) or D2R (Su et al., 2014). Because the observed changes in gene expression and cell fate could all be related to reported effects of increased Wnt signaling, and because DISC1 has been shown to have multiple roles in the Wnt pathway, we next sought to investigate the Wnt signaling properties of *DISC1*-targeted neural progenitors.

DISC1-Disrupted NPCs Display Elevated Baseline Wnt Signaling Activity Independent of Dorsal Identity

We investigated canonical Wnt signaling in NPCs derived from our isogenic wild-type and *DISC1*-disrupted iPSCs. We evaluated Wnt signaling by introducing a T cell factor (TCF)/(lymphoid enhancer factor (LEF)-responsive luciferase (Super8xTOPFLASH) into cells by Amaxa nucleofection, followed by incubation with control (L) or Wnt3a (W) conditioned media (CM) for 24 hr. Analysis of luciferase activity in cell lysates showed that *DISC1*-disrupted NPCs displayed decreased Wnt responsiveness, with a smaller fold change in luciferase activity after Wnt3a application relative to control NPCs (Figure 6C). However, this decreased Wnt response is driven by increased baseline Wnt signaling in DISC1-disrupted cells (WT versus DISC1 mutant L CM luciferase activity; Figure 6B). Interestingly, this phenotype is not present in iPSCs (Figure S5), highlighting the cell fate specificity of this DISC1-mediated alteration in Wnt signaling. These results suggest that *DISC1* disruption decreases the Wnt response in human telencephalic NPCs by increasing basal Wnt signaling.

We next explored the functional consequences of the observed increase in baseline Wnt signaling with *DISC1* disruption by examining NPC proliferation in wild-type and *DISC1* exon 8 WT/mut cells. 5-Ethynyl-2′-deoxyuridine (EdU) incorporation showed an increase in the basal proliferation rate of exon 8 WT/mut NPCs relative to wild-type cells (Figures 6D and 6E). These studies suggest that the increased baseline luciferase Wnt signaling activity in *DISC1*-disrupted NPCs results in increased baseline neural progenitor proliferation.

The fate-related gene expression changes and increased baseline Wnt signaling observed in *DISC1*-disrupted cells could be related or independent phenotypes. Altered cell fate could modify Wnt signaling by changing the pool of cells being assayed, increased baseline Wnt signaling could alter cell fate, or altered Wnt signaling and cell fate could be interrelated in a more complex manner. If dorsal NPC fates have different intrinsic Wnt signaling properties than more ventral NPCs, then changes in Wnt signaling may be observed in dorsally shifted NPCs. To assess whether the observed alteration in Wnt signaling could be induced in wild-type cells by forcing a dorsal fate, we pushed NPCs to more dorsal fates by antagonizing Shh signaling with cyclopamine during days 5–17 of differentiation (Chen et al., 2002; Wen et al., 2014). NPCs were rosette-selected and cultured as neural aggregates without cyclopamine for ~13 days prior to Wnt signaling assays (Figure 6A). Cyclopamine pretreatment did not alter baseline levels of Wnt signaling or Wnt responsiveness in wild-type or *DISC1*-disrupted NPCs (Figures 6F and 6G). In parallel with Wnt assays, dissociated NPCs were plated and differentiated as neurons for 16 days, followed by RNA harvest. NanoString showed that a window of prior cyclopamine exposure did not alter the expression of many cell fate markers, supporting previous studies demonstrating the default dorsal fate of NPCs differentiated from human pluripotent cells (Espuny-Camacho et al., 2013; Kim et al., 2011; Li et al., 2009). Cyclopamine treatment did decrease FoxG1 expression in wild-type cells (Figure 6H), suggesting that decreased *FoxG1* expression in *DISC1*-disrupted cells can be mimicked in wild-type cells using cyclopamine to dorsalize NPCs. However, the increased baseline Wnt signaling and decreased Wnt-responsiveness of *DISC1*-disrupted NPCs is not induced in wild-type cells with cyclopamine treatment. Therefore, shifting cells to a more dorsal identity is not sufficient to induce the altered Wnt signaling seen in *DISC1*-disrupted cells.

Wnt Signaling and Gene Expression Changes in *DISC1*-Disrupted Cells Can Be Rescued with Wnt Antagonism in a Critical Window of Neurodevelopment

The elevation in baseline canonical Wnt signaling in *DISC1*-disrupted NPCs suggested an alternate mechanism whereby *DISC1* interruption alters cell fate via increased Wnt signaling. To test this hypothesis, we treated wild-type and *DISC1* exon 8 WT/mut NPCs with either a Wnt agonist (CHIR99021 [CHIR]) or antagonist (XAV939 [XAV]) during days 7–17 of differentiation. Immunostaining of NPCs showed dramatic morphological and gene expression changes with CHIR99021 treatment, including decreased FoxG1 and Tbr2 expression and increased MAP2 expression, whereas XAV treatment had no qualitative effects on immunostaining of neural markers (Figure 7A). Neural rosettes were then cultured in suspension as neural aggregates in the absence of small molecules prior to assaying Wnt signaling. Prior Wnt agonism caused wild-type cells to mimic the decreased Wnt responsiveness of *DISC1*-targeted cells (Figure 7C). CHIR99021 treatment also caused a dramatic decrease in Wnt baseline signaling, likely because of the observed decrease in NPCs and increase in premature neuronal differentiation (Figures 7A and 7B). In contrast, prior Wnt antagonism with XAV939 decreased baseline Wnt signaling and increased Wnt

(G and H) Quantification of western blots for SYP (G) and SYN I (H) in day 40 neuronal lysates, normalized to Tau (similar results were observed with normalization to MAP2 and GAPDH).

(I) Representative western blot of the neuronal markers SYN I, SYP, MAP2, and Tau and the loading control GAPDH in day 40 neuronal lysates. These are the same samples as those shown in Figure 2D (GAPDH is shown in both for reference).

Data were derived from at least eight independent differentiations. Statistics: two-way ANOVA (D–F) and one-way ANOVA (G and H). Mean ± SEM is shown. *p < 0.05, **p < 0.01, ***p < 0.001, ****p < 0.0001.

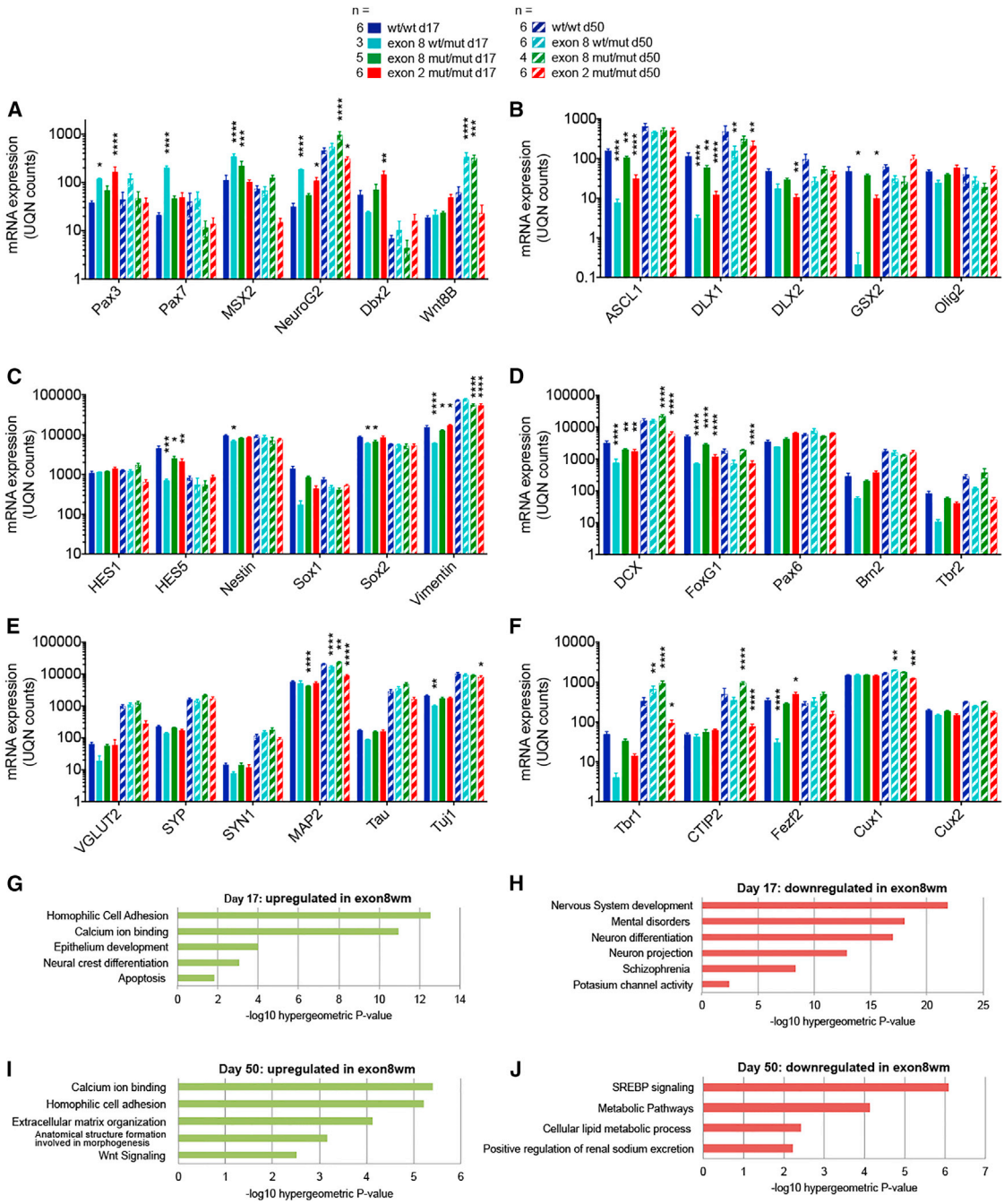

Figure 5. RNA-Seq Supports a Dorsal Fate Shift in *DISC1*-Targeted NPCs and Neurons

iPSCs were differentiated to NPCs (day 17) and neurons (day 50), and RNA was harvested for RNA-seq. Counts were upper quartile-normalized.

(A–F) Expression of selected (A) dorsal telencephalic markers, (B) ventral telencephalic markers, (C and D) NPC markers, and (E and F) neuronal markers. Statistics are shown versus the WT of the corresponding differentiation day. Data were derived from two to six independent differentiations. Statistics: two-way ANOVA. Mean ± SEM is shown. *p < 0.05, **p < 0.01, ***p < 0.001, ****p < 0.0001.

(G–J) Gene ontology analysis of exon 8 WT/mut versus WT/WT day 17 (G and H) and day 50 (I and J) cells.

See also Figure S4.

responsiveness in *DISC1* exon 8 WT/mut NPCs (Figures 7B and 7C). The altered Wnt response of *DISC1*-targeted NPCs can therefore be rescued by prior Wnt antagonism during a 10-day window early in neural development.

Concurrent with Wnt signaling assays, NPCs were plated and differentiated as neurons for 16 days, followed by RNA harvest and gene expression analyses. Antagonizing NPC Wnt signaling with XAV939 rescued decreased *FoxG1*, *Brn2*, and *Tbr2*

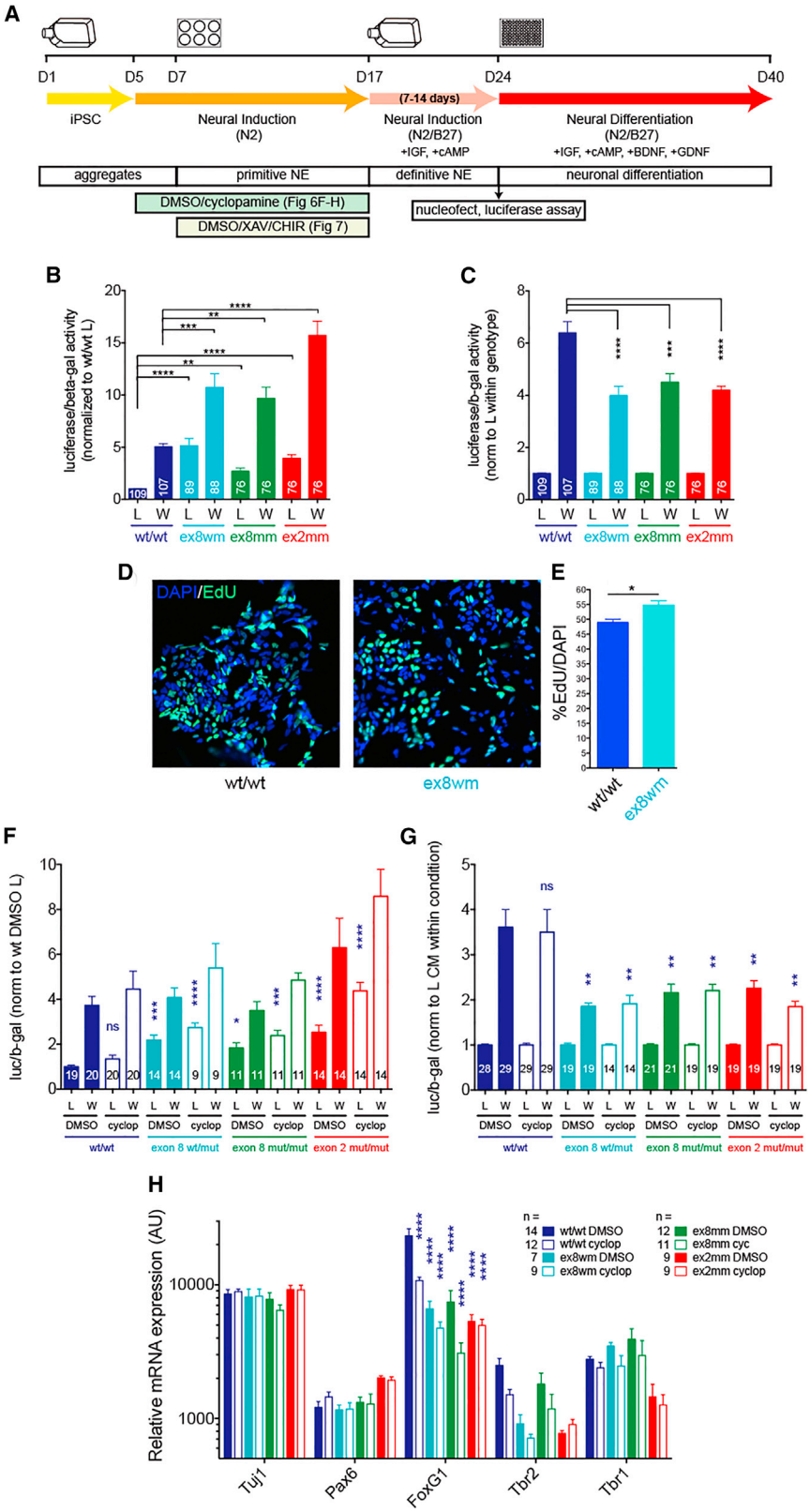

Figure 6. *DISC1* Interruption Increases Basal Wnt Signaling and Decreases Wnt Responsiveness in NPCs Independent of Shh Antagonism

(A) Schematic of the experimental design. iPSC-derived day 24 NPCs were nucleofected with plasmids encoding the Super8XTOPFlash luciferase reporter and pMIR-REPORT-β-galactosidase as a marker of transfection efficiency. After 18 hr, media were changed to control (L) or Wnt3a (W) CMs for 24 hr, followed by cell lysis. IGF, insulin-like growth factor; BDNF, brain-derived neurotrophic factor; GDNF, glial cell-derived neurotrophic factor; NE, neuroepithelium.

(B–E) Cell lysate luciferase activity was normalized to β-galactosidase activity and WT/WT L levels (B), L levels within genotype (C), WT/WT DMSO L levels (D), or L levels within condition (E).

(B and C) *DISC1* disruption causes increased baseline Wnt signaling (B), which drives the decreased Wnt response (C).

(D and E) *DISC1* interruption increases baseline NPC proliferation. NPCs were cultured in control CM for 24 hr, followed by addition of 10 μM EdU for 4 hr and EdU withdrawal for 4 hr.

(D) Example images of EdU and DAPI.

(E) Quantification of percent EdU/DAPI. Data were derived from four independent differentiations.

(F and G) Wild-type and DISC1-disrupted cells treated with vehicle (DMSO) or cyclopamine (cyclop) to dorsalize NPCs for days 5–17 do not alter baseline Wnt signaling (F) or the Wnt response (G). Statistics in (F) are shown versus WT DMSO L. Statistics in (G) are shown versus WT DMSO W. Sample numbers are shown in the columns.

(H) RNA was harvested from day 40 neurons and used for NanoString. Gene expression was normalized to all genes. Statistics are shown versus WT DMSO.

Mean ± SEM is shown. Data were derived from at least three independent differentiations. Statistics: one-way ANOVA (B–G) and two-way ANOVA (H). *p < 0.05, **p < 0.01, ***p < 0.001, ****p < 0.0001.

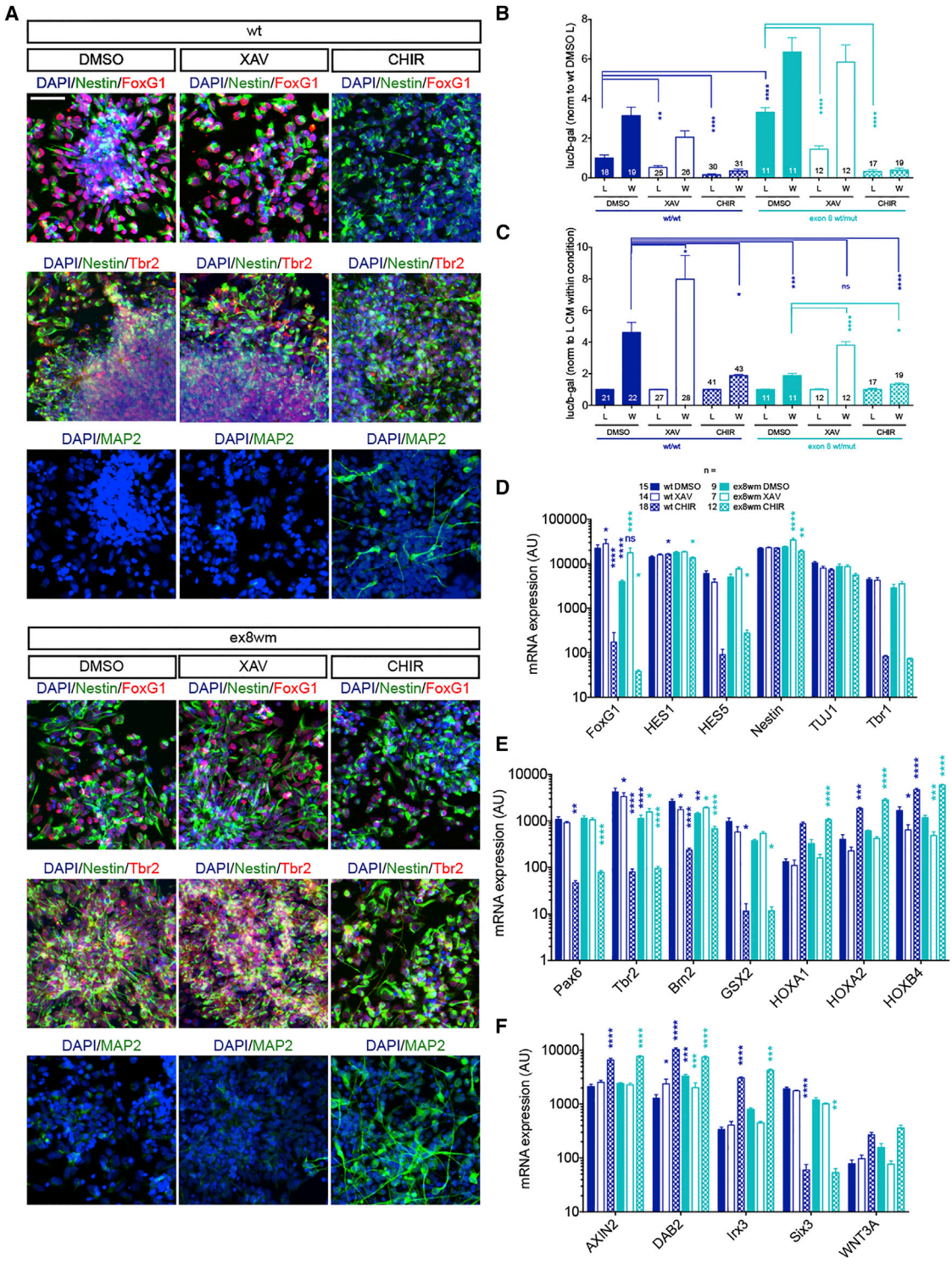

Figure 7. Wnt Antagonism in a Critical Early Window Rescues Altered Wnt Signaling and Cell Fate in *DISC1*-Disrupted Cells

iPSCs were differentiated to NPCs and treated with vehicle (DMSO), the Wnt antagonist XAV939, or the Wnt agonist CHIR during days 7–17. After rosette selection on day 17, small molecules were withdrawn.

(A) Examples of immunostained NPCs (day 19) are shown. Scale bar, 50 um.

(B and C) Prior exposure to Wnt, the antagonist XAV939 decreases baseline Wnt signaling and increases Wnt responsiveness in NPCs, whereas the Wnt agonist CHIR99021 decreases Wnt responsiveness. iPSC-derived NPCs were nucleofected with plasmids encoding the Super8XTOPFlash luciferase reporter and

(legend continued on next page)

expression in exon 8 WT/mut neurons (Figures 7D and 7E). XAV939 also rescued increased *DAB2* expression in exon 8 WT/mut cells, whereas CHIR99021 increased *DAB2* levels in WT and exon 8 WT/mut neurons (Figure 7F).

Stimulating Wnt signaling with CHIR99021 pushed NPCs to differentiate spontaneously, decreasing the expression of progenitor markers and cortical layer markers (Figures 7D and 7E). CHIR99021 treatment also resulted in decreased expression of the ventral marker *GSX2* and increased expression of the caudal genes *HOXA1/2* and *HOXB4*, consistent with the effects of Wnt in dorsal and posterior patterning (Figure 7E). Furthermore, prior treatment of NPCs with CHIR99021 altered neuronal expression of the Wnt pathway genes *AXIN2*, *Irx3*, and *Six3* (Figure 7F). The reversal of gene expression changes in exon 8-targeted neurons with Wnt antagonism during NPC development suggests that altered cell identity in *DISC1*-disrupted cells is downstream of increased Wnt signaling. Wnt antagonism in *DISC1* exon 8 WT/mut cells also rescued increased baseline Wnt signaling and decreased Wnt responsiveness in *DISC1*-targeted NPCs. These studies support a model in which altered Wnt signaling and cell identity are interdependent phenotypes in *DISC1*-disrupted NPCs and neurons (Figure S6).

DISCUSSION

The study of genetic predispositions to mental illness, even if found only in a small subset of patients, will improve our understanding of the pathophysiology of these debilitating disorders. Both rare, highly penetrant and common, weaker *DISC1* variants have been associated with multiple MMIs (reviewed in Brandon and Sawa, 2011). The Scottish chr(1;11) translocation provides an opportunity to investigate the pathophysiology of a rare genetic alteration that has been strongly linked to MMI (Porteous et al., 2014). Animal models have identified critical neurodevelopmental roles for DISC1 (Brandon and Sawa, 2011). Because of differences in *DISC1* splicing between human and rodent samples (Ma et al., 2002; Nakata et al., 2009) as well as the evolutionary divergence in the development of the cerebral cortex, there is a need to complement animal models with studies of human neurons and glia. Furthermore, although DISC1 has been shown to function in a myriad of pathways, studies such as ours prioritize the developmental phenotypes relevant to increasing risk for MMIs.

It is important to keep in mind that patients with MMI, with or without DISC1 disruption, do not show dramatic morphological alterations in the brain and do not show global neuronal dysfunction. To identify relatively subtle developmental defects and to attribute these to a particular mutation, it may be necessary to generate isogenic lines and interrogate multiple lines over several differentiations with high numbers of wells. To investigate the consequences of *DISC1* interruption in human neurons with a controlled genetic background, we TALEN- and CRISPR-Cas9-targeted iPSCs. We found that genomic *DISC1* interruption near the site of the Scottish chr(1;11) translocation causes loss of expression of longer *DISC1* transcripts from the mutated allele by NMD, which increases baseline Wnt signaling and alters the transcriptional profile of NPCs and neurons. These data support a loss-of-function model in which *DISC1* interruption causes decreased full-length DISC1 expression and has downstream developmental consequences.

The limited evidence that exists from t(1;11) patients suggests that the translocation lowers DISC1 transcript and protein levels in patient-derived non-neuronal cells (Millar et al., 2005). Based on the genomic structure surrounding the t(1;11) breakpoint, if splicing occurs between *DISC1* exon 8 and the next available exon on chr11, then the resulting transcript would contain a PTC prior to the last exon of the chr11 gene. This fusion transcript should therefore also recruit the NMD pathway, as observed in our exon 8 mutant model. The common effect of exon 8 1-bp insertion or deletion on decreasing *DISC1* expression suggests that the number of codons (3 or 27) preceding the PTC does not alter targeting of the transcript for NMD. The exon 2 mutant lines demonstrate that an independent *DISC1* mutation can dysregulate many of the same processes as our disease-relevant exon 8 disruption and has even stronger effects on neuronal cell identity. The phenotypes observed in exon 2 lines may result from a loss of long DISC1 isoforms and/or expression of the truncated protein. Because exon 2 mutation does not dramatically alter *DISC1* transcript structure by RNA-seq (Figure S4A), we hypothesize that the truncated DISC1 protein may result from forced use of an alternate start codon downstream of the introduced frameshift mutation. It should be noted that, because we have not generated the chr(1;11) translocation, we could not assess for the presence of a fusion transcript, evaluate the effects of disruption of the antisense long non-coding RNA (lncRNA) *DISC2*, or assess for alterations in expression of translocation-adjacent genes. In patients carrying t(1;11), there has been no evidence of expression of a truncated DISC1 or a DISC1 fusion protein with the nearest downstream chromosome 11 gene (*DISC1FP1* or *Boymaw*) (Millar et al., 2005). However, there is evidence of expression of a fusion protein of DISC1 with the upstream gene, translin-associated factor X (*TSNAX/TRAX*), in the brain (Millar et al., 2000). The balanced translocation may affect expression of this protein in a manner that is not recapitulated with our engineered mutations.

pMIR-REPORT-β-galactosidase as a marker of transfection efficiency. After 18 hr, media were changed to control (L) or Wnt3a (W) CMs for 24 hr, followed by cell lysis. Cell lysate luciferase activity (luc) was normalized to β-galactosidase activity (b-gal) and WT/WT DMSO L levels (B) or L levels within the treatment condition (C). Sample numbers are shown in the columns.

(D–F) RNA was harvested from day 40 neurons and used for NanoString.

(D and E) Expression of selected progenitor and neuronal, dorsal, ventral, and caudal markers.

(F) Expression of Wnt pathway genes.

Gene expression was normalized to all genes. Significance asterisks in dark blue are versus WT/WT DMSO, and asterisks in light blue are versus ex8wm DMSO. All luciferase assay and NanoString samples were independent of samples used in Figure 6. Mean ± SEM is shown. Data were derived from at least three independent differentiations. Statistics: one-way ANOVA (B and C) and two-way ANOVA (D–F). *$p < 0.05$, **$p < 0.01$, ***$p < 0.001$, ****$p < 0.0001$.

The results described here reveal a role of *DISC1* disruption in disordered neurodevelopment. Previous analyses of sporadic psychiatric disease with human iPSCs have also shown changes in neural development (Brennand et al., 2011, 2015; Yu et al., 2014). Another study used iPSCs with a distinct *DISC1* mutation found in an American family in which a 4-bp deletion in exon 12 co-segregates with schizophrenia (Sachs et al., 2005; Wen et al., 2014). Although the causality of this mutation remains unclear based on pedigree size and identification of the mutation in control subjects (Green et al., 2006), this mutation resulted in dysregulation of presynaptic biology, including increased presynaptic protein expression in cortical neurons (Wen et al., 2014). We did not observe an upregulation of presynaptic proteins with exon 8 or exon 2 *DISC1* interruption. The differentiation methods used in that study included the use of dual SMAD inhibition and cyclopamine, which likely generates a different population of neural progenitors and neurons, which, in turn, may alter the resulting neuronal phenotypes (Hébert and Fishell, 2008). Interestingly, although the phenotypes described are divergent between our studies, a common subset of genes is dysregulated with the two models (Figure S4F). Future studies with these models have the potential to provide a powerful system to identify convergent phenotypes of these disparate DISC1 mutations.

Here we found that disease-relevant *DISC1* disruption alters canonical Wnt signaling in human NPCs, as assessed by TCF/LEF-driven gene expression. We observed that *DISC1* disruption decreases Wnt responsiveness in human NPCs, consistent with the decreased Wnt response upon *DISC1* knockdown in murine NPCs (Mao et al., 2009). That study suggested a direct role for DISC1 in the Wnt signaling pathway, in which DISC1 binds and inhibits GSK3β. Here we find that that the loss of long DISC1 isoforms drives decreased Wnt responsiveness via elevated baseline Wnt signaling. This difference may result from the use of human versus rodent cells or the use of total DISC1 knockdown versus disease-relevant loss of long DISC1 transcripts or may suggest a different role for DISC1 in the Wnt signaling pathway.

The Wnt signaling pathway has been implicated in the pathophysiology of neuropsychiatric disorders, making the role of DISC1 in this pathway of particular interest (Freyberg et al., 2010). We found that *DISC1* disruption causes altered NPC and neuronal gene expression profiles via increased Wnt signaling. Our data are consistent with rodent models in which increased Wnt signaling in the developing brain causes a dorsal NPC fate shift, decreases FoxG1 expression, and decreases Tbr2 expression by promoting IP differentiation (Backman et al., 2005; Munji et al., 2011). Wnt inhibition with XAV939 for a 10-day window in *DISC1*-targeted NPCs rescued changes in neural cell identity, suggesting that increased Wnt signaling with *DISC1*-disruption is upstream of observed gene expression differences. The increase in *Tbr2* expression with XAV939 treatment upholds, and extends to human telencephalic cells, previous reports that Wnt antagonism causes an expansion of Tbr2+ IPs (Fang et al., 2013, 2014; Munji et al., 2011). These studies suggest a model in which *DISC1* interruption increases baseline Wnt signaling, which alters the pool of NPCs, resulting in decreased Wnt responsiveness.

Further work will be required to elucidate the exact mechanism by which *DISC1* disruption alters Wnt signaling and fate-related gene expression profiles in human NPCs. We identified numerous gene expression changes that result from *DISC1* interruption by RNA sequencing, which provide interesting candidates for future study. This study shows the utility of human iPSCs in modeling mental illness-associated defects in human neurodevelopment and strengthens the association between Wnt signaling, neurodevelopment, and major mental illness.

EXPERIMENTAL PROCEDURES

Genome Editing

The healthy control human iPSC line YZ1 was obtained from the University of Connecticut Stem Cell Core (Zeng et al., 2010). TALENs were designed and constructed using a hierarchical ligation procedure (Sanjana et al., 2012). TALE monomer plasmids and TALEN backbone plasmids were a generous gift from Feng Zhang. Exon 8 TALENs were designed targeting unique genomic sequences in DISC1 exon 8. For CRISPR-Cas9 targeting, a unique genomic site in DISC1 exon 2 was cloned into a guide RNA cloning vector. Targeting plasmids were electroporated into dissociated YZ1 iPSCs using the Amaxa 4D-Nucleofector X unit (Lonza). 48 hr after transfection, iPSCs were dissociated, and GFP+ cells were collected by fluorescence-activated cell sorting (FACS). Individual clones were screened for genomic mutation by PCR amplification around the target site, followed by Sanger sequencing.

Neuronal Differentiation

Neuronal differentiation was performed using an embryoid aggregate-based protocol, as described previously (Muratore et al., 2014a, 2014b). For dorsal-ventral patterning, cells were treated with 2 μM cyclopamine (Santa Cruz Biotechnology) or vehicle (DMSO, Sigma) as indicated during days 5–17 of differentiation. For Wnt manipulation, cells were treated with 2 μM XAV939 (Stemgent), 3 μM CHIR99021 (Tocris Bioscience), or vehicle (DMSO), as indicated, during days 7–17 of differentiation. See Supplemental Experimental Procedures for details and media recipes.

qPCR

RNA was reverse-transcribed, and cDNA was used for qPCR with Fast SYBR Green Master Mix (Life Technologies) on a ViiA 7 system (Life Technologies). Data were normalized to glyceraldehyde 3-phosphate dehydrogenase (GAPDH) expression using the $\Delta\Delta C_T$ method as described previously (Livak and Schmittgen, 2001). Primer sequences are listed in the Supplemental Experimental Procedures.

NanoString Gene Expression Analysis

Two 150-gene nCounter Custom CodeSets were designed by NanoString Technologies. One codeset was used to generate initial expression data (Figures 2, 3, and 4; Table S3A). Data were analyzed by subtracting counts from a blank control and normalizing to eight housekeeping genes (B2M, GAPDH, GUSB, HPRT1, LDHA, POLR2A, RPL13a, and RPL27). After this codeset was depleted, another codeset was made that greatly overlapped with the initial codeset. This codeset was used to generate patterning data (Figures 6 and 7; Table S3B). These data were analyzed with nSolver analysis software (NanoString Technologies) and normalized to the total gene set. Assays were performed according to the manufacturer's instructions.

Immunocytochemistry and Microscopy

Cells were fixed with 4% paraformaldehyde (Sigma), followed by membrane permeabilization and blocking with 0.2% Triton X-100 (Sigma) and 2% donkey serum (Jackson ImmunoResearch Laboratories). All quantifications were performed blinded to genotype using the Cell Counter plugin in

FIJI. See the Supplemental Experimental Procedures for a list of antibodies used.

Western Blots

Lysates were prepared in a buffer containing 1% NP40, 10 mM EDTA, 150 mM NaCl, 50 mM Tris, complete protease inhibitors, and phosSTOP (Roche). Equal protein amounts were loaded onto 4%–12% Bis-Tris NuPAGE gels (Life Technologies) and transferred to nitrocellulose membranes for blotting. Antibodies and dilutions are listed in the Supplemental Experimental Procedures.

RNA Sequencing

RNA was extracted from day 17 or day 50 samples. Total RNA was converted into cDNA libraries using the TruSeq Stranded Total RNA-RiboZero Gold sample prep kit (Illumina). RNA was sequenced on an Illumina HiSeq using stranded paired-end reads with ~50 million reads/sample.

Differential Gene Expression Analysis

Reads were mapped to the University of California, Santa Cruz human reference genome (hg19) using TopHat v2.0.10 (Kim et al., 2013). Reads mapping to genes were counted using htseq (v0.6.1) (Anders et al., 2015). Counts were upper quartile-normalized using SVS (Golden Helix) for limited gene comparisons. Alternatively, differential gene expression analysis between lines was performed using the edgeR package in R with a false discovery rate of 0.05 (Robinson et al., 2010).

Luciferase Assays

Control and Wnt3a CMs were produced using Wnt3a-expressing and control (L) cells (ATCC). CMs were generated according to the ATCC protocol. Neural aggregates (~days 27–31) were dissociated using Accutase. Cells were electroporated with Super8XTOPFlash (a gift from Randall Moon) and pMIR-REPORT-β-galactosidase (Life Technologies) using the Amaxa 4D-Nucleofector X unit (Lonza). 16 hr later, the medium was changed to L or Wnt3a CM for 24 hr. Cells were then lysed and used for a firefly luciferase assay (Biotium) and β-galactosidase assay (Promega). Luciferase activity was normalized to β-galactosidase activity for each sample.

EdU Incorporation

Neural aggregates (~days 27–31) were dissociated using Accutase and plated onto poly-ornithine/laminin-coated 96-well plates at 25,000 cells/well. 16 hr later, the medium was changed to L CM for 24 hr. Cells were then incubated in L CM + 10 μM EdU for 4 hr, followed by incubation in L CM (without EdU) for 4 hr. Cells were then fixed as described above, and EdU staining was carried out using a Click-iT EdU imaging kit (Invitrogen).

To quantify the EdU signal, cells were imaged using an IN Cell Analyzer 2000 high-content platform (GE Healthcare). Image sets were analyzed using the multi-target analysis algorithm in the IN Cell Workstation software (GE Healthcare).

Data Collection and Statistics

All data represent at least three independent experiments, with the minimum "n" and number of differentiations listed in each figure or figure legend, and utilizing the iPSC lines as shown in Table S1. Data were analyzed using GraphPad PRISM 6 software. Values are expressed as mean ± SEM. Statistical significance was tested as indicated in the figure legends.

ACCESSION NUMBERS

The accession number for the data reported in this paper is GEO: GSE71289.

SUPPLEMENTAL INFORMATION

Supplemental Information includes Supplemental Experimental Procedures, six figures, and three tables and can be found with this article online at http://dx.doi.org/10.1016/j.celrep.2015.07.061.

AUTHOR CONTRIBUTIONS

P.S. led and was involved in every aspect of the project. D.G.C. assisted with sample preparation, cell culture, and western blots. K.H., J.B., and E.M. assisted with sample preparation and imaging. C.R.M. performed the microelectrode array experiments. M.L., H.Z., and K.K. assisted with RNA-seq analyses. T.L.Y-P., D.J.S., and P.S. designed the project and wrote the manuscript.

ACKNOWLEDGMENTS

We thank N. Sanjana and F. Zhang for help with designing TALENs and providing the TALE monomer and TALEN backbone plasmids; R. Hevner for sharing the Tbr2 antibody; C. Zhou, F. Abawi, and P. Mouradian for technical assistance; and R. Nehme and K. Eggan for valuable feedback. This work is supported by funding from the Sackler Scholar Programme in Psychobiology, NIGMS grant T32GM007753, NIA grant T32AG000222, and NIMH grant 1F30MH103890-01A1 (to P.S.); NIA grant 2R01AG006173-26 (to D.J.S.); and a Young Investigator Award from the Brain and Behavior Research Foundation, the Harvard Stem Cell Institute, and NIMH grants R00MH085004 and R01MH101148 (to T.L.Y.P.). RNA sequencing work was funded by a grant obtained through Expression Analysis (to T.L.Y.P.).

Received: May 21, 2015
Revised: July 8, 2015
Accepted: July 29, 2015
Published: August 20, 2015

REFERENCES

Anders, S., Pyl, P.T., and Huber, W. (2015). HTSeq–a Python framework to work with high-throughput sequencing data. Bioinformatics *31*, 166–169.

Backman, M., Machon, O., Mygland, L., van den Bout, C.J., Zhong, W., Taketo, M.M., and Krauss, S. (2005). Effects of canonical Wnt signaling on dorso-ventral specification of the mouse telencephalon. Dev. Biol. *279*, 155–168.

Blackwood, D.H., Fordyce, A., Walker, M.T., St Clair, D.M., Porteous, D.J., and Muir, W.J. (2001). Schizophrenia and affective disorders–cosegregation with a translocation at chromosome 1q42 that directly disrupts brain-expressed genes: clinical and P300 findings in a family. Am. J. Hum. Genet. *69*, 428–433.

Brandon, N.J., and Sawa, A. (2011). Linking neurodevelopmental and synaptic theories of mental illness through DISC1. Nat. Rev. Neurosci. *12*, 707–722.

Brennand, K.J., Simone, A., Jou, J., Gelboin-Burkhart, C., Tran, N., Sangar, S., Li, Y., Mu, Y., Chen, G., Yu, D., et al. (2011). Modelling schizophrenia using human induced pluripotent stem cells. Nature *473*, 221–225.

Brennand, K., Savas, J.N., Kim, Y., Tran, N., Simone, A., Hashimoto-Torii, K., Beaumont, K.G., Kim, H.J., Topol, A., Ladran, I., et al. (2015). Phenotypic differences in hiPSC NPCs derived from patients with schizophrenia. Mol. Psychiatry *20*, 361–368.

Chen, J.K., Taipale, J., Cooper, M.K., and Beachy, P.A. (2002). Inhibition of Hedgehog signaling by direct binding of cyclopamine to Smoothened. Genes Dev. *16*, 2743–2748.

Cross-Disorder Group of the Psychiatric Genomics Consortium (2013). Identification of risk loci with shared effects on five major psychiatric disorders: a genome-wide analysis. Lancet *381*, 1371–1379.

Danesin, C., Peres, J.N., Johansson, M., Snowden, V., Cording, A., Papalopulu, N., and Houart, C. (2009). Integration of telencephalic Wnt and hedgehog signaling center activities by Foxg1. Dev. Cell *16*, 576–587.

Englund, C., Fink, A., Lau, C., Pham, D., Daza, R.A.M., Bulfone, A., Kowalczyk, T., and Hevner, R.F. (2005). Pax6, Tbr2, and Tbr1 are expressed sequentially by radial glia, intermediate progenitor cells, and postmitotic neurons in developing neocortex. J. Neurosci. *25*, 247–251.

Espuny-Camacho, I., Michelsen, K.A., Gall, D., Linaro, D., Hasche, A., Bonnefont, J., Bali, C., Orduz, D., Bilheu, A., Herpoel, A., et al. (2013). Pyramidal neurons derived from human pluripotent stem cells integrate efficiently into mouse brain circuits in vivo. Neuron *77*, 440–456.

Fang, W.-Q., Chen, W.-W., Fu, A.K.Y., and Ip, N.Y. (2013). Axin directs the amplification and differentiation of intermediate progenitors in the developing cerebral cortex. Neuron *79*, 665–679.

Fang, W.-Q., Chen, W.-W., Jiang, L., Liu, K., Yung, W.-H., Fu, A.K.Y., and Ip, N.Y. (2014). Overproduction of upper-layer neurons in the neocortex leads to autism-like features in mice. Cell Rep. *9*, 1635–1643.

Freyberg, Z., Ferrando, S.J., and Javitch, J.A. (2010). Roles of the Akt/GSK-3 and Wnt signaling pathways in schizophrenia and antipsychotic drug action. Am. J. Psychiatry *167*, 388–396.

Green, E.K., Norton, N., Peirce, T., Grozeva, D., Kirov, G., Owen, M.J., O'Donovan, M.C., and Craddock, N. (2006). Evidence that a DISC1 frame-shift deletion associated with psychosis in a single family may not be a pathogenic mutation. Mol. Psychiatry *11*, 798–799.

Harrison, P.J. (1999). The neuropathology of schizophrenia. A critical review of the data and their interpretation. Brain *122*, 593–624.

Hébert, J.M., and Fishell, G. (2008). The genetics of early telencephalon patterning: some assembly required. Nat. Rev. Neurosci. *9*, 678–685.

Hevner, R.F., Hodge, R.D., Daza, R.A.M., and Englund, C. (2006). Transcription factors in glutamatergic neurogenesis: conserved programs in neocortex, cerebellum, and adult hippocampus. Neurosci. Res. *55*, 223–233.

Hirabayashi, Y., Itoh, Y., Tabata, H., Nakajima, K., Akiyama, T., Masuyama, N., and Gotoh, Y. (2004). The Wnt/beta-catenin pathway directs neuronal differentiation of cortical neural precursor cells. Development *131*, 2791–2801.

Ishigaki, Y., Li, X., Serin, G., and Maquat, L.E. (2001). Evidence for a pioneer round of mRNA translation: mRNAs subject to nonsense-mediated decay in mammalian cells are bound by CBP80 and CBP20. Cell *106*, 607–617.

Johnson, M.B., Wang, P.P., Atabay, K.D., Murphy, E.A., Doan, R.N., Hecht, J.L., and Walsh, C.A. (2015). Single-cell analysis reveals transcriptional heterogeneity of neural progenitors in human cortex. Nat. Neurosci. *18*, 637–646.

Kim, J.-E., O'Sullivan, M.L., Sanchez, C.A., Hwang, M., Israel, M.A., Brennand, K., Deerinck, T.J., Goldstein, L.S.B., Gage, F.H., Ellisman, M.H., and Ghosh, A. (2011). Investigating synapse formation and function using human pluripotent stem cell-derived neurons. Proc. Natl. Acad. Sci. USA *108*, 3005–3010.

Kim, D., Pertea, G., Trapnell, C., Pimentel, H., Kelley, R., and Salzberg, S.L. (2013). TopHat2: accurate alignment of transcriptomes in the presence of insertions, deletions and gene fusions. Genome Biol. *14*, R36.

Lefort, R., Pozueta, J., and Shelanski, M. (2012). Cross-linking of cell surface amyloid precursor protein leads to increased β-amyloid peptide production in hippocampal neurons: implications for Alzheimer's disease. J. Neurosci. *32*, 10674–10685.

Li, X.-J., Zhang, X., Johnson, M.A., Wang, Z.-B., Lavaute, T., and Zhang, S.-C. (2009). Coordination of sonic hedgehog and Wnt signaling determines ventral and dorsal telencephalic neuron types from human embryonic stem cells. Development *136*, 4055–4063.

Livak, K.J., and Schmittgen, T.D. (2001). Analysis of relative gene expression data using real-time quantitative PCR and the 2(-Delta Delta C(T)) Method. Methods *25*, 402–408.

Ma, L., Liu, Y., Ky, B., Shughrue, P.J., Austin, C.P., and Morris, J.A. (2002). Cloning and characterization of Disc1, the mouse ortholog of DISC1 (Disrupted-in-Schizophrenia 1). Genomics *80*, 662–672.

Manuel, M., Martynoga, B., Yu, T., West, J.D., Mason, J.O., and Price, D.J. (2010). The transcription factor Foxg1 regulates the competence of telencephalic cells to adopt subpallial fates in mice. Development *137*, 487–497.

Mao, Y., Ge, X., Frank, C.L., Madison, J.M., Koehler, A.N., Doud, M.K., Tassa, C., Berry, E.M., Soda, T., Singh, K.K., et al. (2009). Disrupted in schizophrenia 1 regulates neuronal progenitor proliferation via modulation of GSK3beta/beta-catenin signaling. Cell *136*, 1017–1031.

Martynoga, B., Morrison, H., Price, D.J., and Mason, J.O. (2005). Foxg1 is required for specification of ventral telencephalon and region-specific regulation of dorsal telencephalic precursor proliferation and apoptosis. Dev. Biol. *283*, 113–127.

Millar, J.K., Wilson-Annan, J.C., Anderson, S., Christie, S., Taylor, M.S., Semple, C.A., Devon, R.S., St Clair, D.M., Muir, W.J., Blackwood, D.H., and Porteous, D.J. (2000). Disruption of two novel genes by a translocation co-segregating with schizophrenia. Hum. Mol. Genet. *9*, 1415–1423.

Millar, J.K., Pickard, B.S., Mackie, S., James, R., Christie, S., Buchanan, S.R., Malloy, M.P., Chubb, J.E., Huston, E., Baillie, G.S., et al. (2005). DISC1 and PDE4B are interacting genetic factors in schizophrenia that regulate cAMP signaling. Science *310*, 1187–1191.

Mitchell, K.J. (2011). The genetics of neurodevelopmental disease. Curr. Opin. Neurobiol. *21*, 197–203.

Molyneaux, B.J., Arlotta, P., Menezes, J.R.L., and Macklis, J.D. (2007). Neuronal subtype specification in the cerebral cortex. Nat. Rev. Neurosci. *8*, 427–437.

Munji, R.N., Choe, Y., Li, G., Siegenthaler, J.A., and Pleasure, S.J. (2011). Wnt signaling regulates neuronal differentiation of cortical intermediate progenitors. J. Neurosci. *31*, 1676–1687.

Muratore, C.R., Rice, H.C., Srikanth, P., Callahan, D.G., Shin, T., Benjamin, L.N.P., Walsh, D.M., Selkoe, D.J., and Young-Pearse, T.L. (2014a). The familial Alzheimer's disease APPV717I mutation alters APP processing and Tau expression in iPSC-derived neurons. Hum. Mol. Genet. *23*, 3523–3536.

Muratore, C.R., Srikanth, P., Callahan, D.G., and Young-Pearse, T.L. (2014b). Comparison and optimization of human iPSC neuronal differentiation protocols. PLoS ONE *9*, e105807.

Nakata, K., Lipska, B.K., Hyde, T.M., Ye, T., Newburn, E.N., Morita, Y., Vakkalanka, R., Barenboim, M., Sei, Y., Weinberger, D.R., and Kleinman, J.E. (2009). DISC1 splice variants are upregulated in schizophrenia and associated with risk polymorphisms. Proc. Natl. Acad. Sci. USA *106*, 15873–15878.

Porteous, D.J., Thomson, P.A., Millar, J.K., Evans, K.L., Hennah, W., Soares, D.C., McCarthy, S., McCombie, W.R., Clapcote, S.J., Korth, C., et al. (2014). DISC1 as a genetic risk factor for schizophrenia and related major mental illness: response to Sullivan. Mol. Psychiatry *19*, 141–143.

Ripke, S., O'Dushlaine, C., Chambert, K., Moran, J.L., Kähler, A.K., Akterin, S., Bergen, S.E., Collins, A.L., Crowley, J.J., Fromer, M., et al.; Multicenter Genetic Studies of Schizophrenia Consortium; Psychosis Endophenotypes International Consortium; Wellcome Trust Case Control Consortium 2 (2013). Genome-wide association analysis identifies 13 new risk loci for schizophrenia. Nat. Genet. *45*, 1150–1159.

Robinson, M.D., McCarthy, D.J., and Smyth, G.K. (2010). edgeR: a Bioconductor package for differential expression analysis of digital gene expression data. Bioinformatics *26*, 139–140.

Sachs, N.A., Sawa, A., Holmes, S.E., Ross, C.A., DeLisi, L.E., and Margolis, R.L. (2005). A frameshift mutation in Disrupted in Schizophrenia 1 in an American family with schizophrenia and schizoaffective disorder. Mol. Psychiatry *10*, 758–764.

Sanjana, N.E., Cong, L., Zhou, Y., Cunniff, M.M., Feng, G., and Zhang, F. (2012). A transcription activator-like effector toolbox for genome engineering. Nat. Protoc. *7*, 171–192.

Schizophrenia Working Group of the Psychiatric Genomics Consortium (2014). Biological insights from 108 schizophrenia-associated genetic loci. Nature *511*, 421–427.

Sessa, A., Mao, C.-A., Hadjantonakis, A.-K., Klein, W.H., and Broccoli, V. (2008). Tbr2 directs conversion of radial glia into basal precursors and guides neuronal amplification by indirect neurogenesis in the developing neocortex. Neuron *60*, 56–69.

Shimamura, K., Hartigan, D.J., Martinez, S., Puelles, L., and Rubenstein, J.L. (1995). Longitudinal organization of the anterior neural plate and neural tube. Development *121*, 3923–3933.

Silva, A.L., and Romão, L. (2009). The mammalian nonsense-mediated mRNA decay pathway: to decay or not to decay! Which players make the decision? FEBS Lett. *583*, 499–505.

St Clair, D., Blackwood, D., Muir, W., Carothers, A., Walker, M., Spowart, G., Gosden, C., and Evans, H.J. (1990). Association within a family of a balanced autosomal translocation with major mental illness. Lancet *336*, 13–16.

Su, P., Li, S., Chen, S., Lipina, T.V., Wang, M., Lai, T.K.Y., Lee, F.H.F., Zhang, H., Zhai, D., Ferguson, S.S.G., et al. (2014). A dopamine D2 receptor-DISC1

protein complex may contribute to antipsychotic-like effects. Neuron *84*, 1302–1316.

Sullivan, P.F., Daly, M.J., and O'Donovan, M. (2012). Genetic architectures of psychiatric disorders: the emerging picture and its implications. Nat. Rev. Genet. *13*, 537–551.

Tao, W., and Lai, E. (1992). Telencephalon-restricted expression of BF-1, a new member of the HNF-3/fork head gene family, in the developing rat brain. Neuron *8*, 957–966.

Taylor, M.S., Devon, R.S., Millar, J.K., and Porteous, D.J. (2003). Evolutionary constraints on the Disrupted in Schizophrenia locus. Genomics *81*, 67–77.

Ulloa, F., and Martí, E. (2010). Wnt won the war: antagonistic role of Wnt over Shh controls dorso-ventral patterning of the vertebrate neural tube. Dev. Dyn. *239*, 69–76.

Vieira, S.I., Rebelo, S., Esselmann, H., Wiltfang, J., Lah, J., Lane, R., Small, S.A., Gandy, S., da Cruz E Silva, E.F., and da Cruz E Silva, O.A. (2010). Retrieval of the Alzheimer's amyloid precursor protein from the endosome to the TGN is S655 phosphorylation state-dependent and retromer-mediated. Mol. Neurodegener. *5*, 40.

Weinberger, D.R. (1995). From neuropathology to neurodevelopment. Lancet *346*, 552–557.

Wen, Z., Nguyen, H.N., Guo, Z., Lalli, M.A., Wang, X., Su, Y., Kim, N.-S., Yoon, K.-J., Shin, J., Zhang, C., et al. (2014). Synaptic dysregulation in a human iPS cell model of mental disorders. Nature *515*, 414–418.

Williams, H.J., Owen, M.J., and O'Donovan, M.C. (2009). Schizophrenia genetics: new insights from new approaches. Br. Med. Bull. *91*, 61–74.

Xuan, S., Baptista, C.A., Balas, G., Tao, W., Soares, V.C., and Lai, E. (1995). Winged helix transcription factor BF-1 is essential for the development of the cerebral hemispheres. Neuron *14*, 1141–1152.

Yu, D.X., Di Giorgio, F.P., Yao, J., Marchetto, M.C., Brennand, K., Wright, R., Mei, A., McHenry, L., Lisuk, D., Grasmick, J.M., et al. (2014). Modeling hippocampal neurogenesis using human pluripotent stem cells. Stem Cell Reports *2*, 295–310.

Zeng, H., Guo, M., Martins-Taylor, K., Wang, X., Zhang, Z., Park, J.W., Zhan, S., Kronenberg, M.S., Lichtler, A., Liu, H.-X., et al. (2010). Specification of region-specific neurons including forebrain glutamatergic neurons from human induced pluripotent stem cells. PLoS ONE *5*, e11853.